5-2021

Using Zebrafish as a Model System for Studying the Autism Risk Gene adnp in Early Embryonic Development

William Theune
University of New Haven

THE UNIVERSITY OF NEW HAVEN

Department of Biology and Environmental Science

Using Zebrafish as a Model System for Studying the Autism Risk Gene *adnp* in Early Embryonic Development

A THESIS

Submitted in partial fulfilment

of the requirements for the degree of

MASTER OF SCIENCE IN CELLULAR AND MOLECULAR BIOLOGY

BY:

William C. Theune
Carter M. Takacs, PhD.
University of New Haven
Department of Biology and Environmental Science
Cellular and Molecular Biology Graduate Program
300 Boston Post Road
West Haven, CT 06516

Using Zebrafish as a Model System for Studying the Autism Risk Gene *adnp* in Early Embryonic Development

APPROVED BY:

Carter Takacs, Ph.D.

Thesis Advisor

Anna Kloc, Ph.D.

Committee Member

Ellen J. Hoffman, MD, Ph.D.

Committee Member

Amy L. Carlile, PhD.

Associated Professor and Chair, Biology and Environmental Science

Shaily Menon, Ph.D.

Dean of the College of Arts and Sciences

Mario Thomas Gaboury, J.D., Ph.D.

Interim Provost & Senior Vice President for Academic Affairs

ACKNOWLEDGMENTS

I would first like to thank my Principal Investigator of over 3 years, Dr. Carter M. Takacs, without whom I never would have discovered my love for developmental biology. Dr. Takacs has been an incredible source of support and expertise throughout my time at the University of New Haven and is someone I am very proud to call my mentor and friend. I would like to thank my Committee Member, Dr. Anna Kloc, for her guidance and support in both my research and academic/career aspirations, which has proven invaluable during my time here at UNH. I would like to thank my Committee Member Dr. Ellen J. Hoffman for her expertise in developmental biology and autism spectrum disorders and for the opportunity to collaborate with her and her lab throughout this project. I would like to thank the University of New Haven Department of Biology & Environmental Science for the ability to conduct this research and for their support. I would also like to thank the NASA Connecticut Space Grant Consortium, for their support and for the chance to work as a graduate research fellow.

ABSTRACT

Autism Spectrum Disorders (ASD) are a group of debilitating neurodevelopmental disorders, estimated to affect 1 in 54 children. Despite the identification of many autism-risk genes, the underlying mechanisms for ASD remain unclear.

One of the most common forms of ASD is associated with *de novo* mutations in the *ADNP* gene (*Activity-Dependent Neuroprotector Homeobox*; accounting for 0.17% of ASD individuals). Termed ADNP syndrome, this disorder is characterized by intellectual disability, facial dysmorphia, and is comorbid with multiple organ system deficits.

We set out to use zebrafish as a model organism to gain mechanistic insights into ADNP function. Zebrafish have the advantage of being high throughput, and have been established as a model for studying behavioral phenotypes and performing drug screenings in larvae. Zebrafish have two paralogs of *adnp*; *adnpa* and *adnpb*. This work characterizes the spatial and temporal expression of *adnpa/b* during zebrafish embryonic development, and details the establishment of a CRISPR/cas9 knockout line for *adnpa/b* in zebrafish. This work also presents preliminary data on CRISPR/Cas13d knockdown of *adnpa* and improvements in the efficiency of cas13d RNA knockdown. Future work aims to study the morphological and behavioral consequences of *adnpa/b* loss of function, as well as the molecular mechanisms by which *adnpa/b* impact zebrafish embryonic development.

CONTENTS

LIST OF FIGURES

INTRODUCTION

Introduction

Autism Spectrum Disorders (ASD) are a classification of developmental disorders which are characterized by intellectual disability, difficulties with social interaction, impairments in verbal and nonverbal communication, and restricted repetitive behaviors[1,2]. ASD affects as many as 1 in every 54 children worldwide and is an incredibly complex and genetically diverse group of disorders[1,3].

Despite numerous autism risk genes being discovered, in 70% of ASD cases the underlying genetic cause is unknown[4]. In recent years, genome-wide association studies (GWAS) have been conducted within autism patient cohorts to elucidate the clinical prevalence of autism-associated mutations. Many autism risk genes have been shown to affect cellular pathways critical for embryonic development, including mTOR, MAPK, and Wnt signaling[5,6]. It is estimated that 500-1000 genes are associated with ASD, with a single gene being responsible for less than 1% of ASD cases[7].

One of the most common forms of ASD is Helsmoortel Van der Aa syndrome or ADNP syndrome[8]. This disorder is characterized by intellectual disability, facial dysmorphia and is frequently comorbid with multiple organ deficits, including brain abnormalities, visual problems, congenital heart defects, gastrointestinal problems and hormonal deficiencies[1,9]. ADNP syndrome is caused by *de novo* mutations in the ADNP gene; and is believed to occur in at least 0.17% of ASD patients; making it one of the most common ASD associated genes[1]. A recent exome sequencing study placed ADNP in the top 5 most prevalent mutated genes in ASD progression[10]. In addition to ASD, ADNP has been implicated in the progression of Alzheimer's

disease and dysregulation with its sister protein ADNP2 has been associated with the development of schizophrenia[11,12].

ADNP encodes the Activity-Dependent Neuroprotector homeobox protein; a transcription factor which has been shown to regulate over 400 genes during embryonic development, related to organogenesis, neurogenesis, heart development and erythropoiesis [13,14,15]. ADNP is a neuroprotective protein which is essential for neural tube closure and in protecting damaged nerve cells from cell death by inducing glial-derived survival promoting substances[16,17]. ADNP silencing leads to increased expression of p53 in neurons; suggesting that ADNP's neuroprotective capability occurs at least in part through inhibition of p53, leading to a reduction in cellular apoptosis in damaged neurons[18]. A subsequent study found that the addition of an ADNP derived drug (NAP) to cells exposed to oxidative stress protected the cells from increases in p53 expression normally associated with the treatment[11].

In mouse models, complete deficiency of ADNP was demonstrated to be embryonic lethal due to cranial neural tube closure failure and death at E-8.5-9.0. Consistent with these findings, the authors also showed that *adnp* is highly expressed during early gestation, peaking at E9.5[19]. Heterozygous mice also show a slight developmental delay[13]. In a study which evaluated the behavioral and intellectual defects of ADNP heterozygous mice, NAP was found to partially rescue cognitive deficits and reduce tau hyperphosphorylation, suggesting that it may be a potential treatment for Alzheimer's and *adnp*-associated intellectual disabilities[17].

A clinical study of patients with Helsmoortel Van der Aa syndrome found that all patients had frameshift mutations in *adnp* leading to a loss of a minimum of 166 amino acids in the C-terminus of the protein[1,20]. It has been hypothesized that the loss of this region of the protein inhibits ADNP from recruiting components of the BAF chromatin remodeling complex[1].

Inhibition of this function might be responsible for the dominant negative effect observed in ADNP syndrome as the mutant copy would competitively inhibit the binding of wild-type ADNP to target DNA sequences[1].

ADNP's roles as a transcription factor and chromatin remodeler as part of the BAF complex, represents a common mechanism for many ASD-risk genes. ADNP interacts with several other ASD risks genes, such as the BAF components ARID1B, and SMARCC2[6]. ADNP's expression is induced downstream of activation of the N-methyl-D-aspartate receptor, of which several subunits, namely, GRIN1 and GRIN2B have been implicated in ASD[6,21]. Thus, the study of ADNP may be applicable to furthering the understanding of basic mechanisms for multiple autism-risk genes.

An effective method for *in vivo* investigation of novel autism associated genes is the zebrafish model organism. Zebrafish are transparent during early development and have short generation times making them an excellent model for developmental and genetic analysis[22]. Additionally, they are highly similar to humans on a genetic level, sharing 70 percent of protein-coding genes[22,23]. Many mutations identified in zebrafish mimic those in human disease, allowing for the identification of medically relevant phenotypes during embryogenesis[22].

Zebrafish have two paralogs of *adnp*; *adnpa* and *adnpb*. The two paralogs share 49.55% sequence similarity and contain many of the same predicted protein domains including C2H2 zinc finger domains, and a homeobox domain. While morpholino knockdown of *adnp* in zebrafish has implicated these two proteins in erythropoiesis, additional research is needed to characterize the expression and study the functional role of these proteins, as well as the effect of mutations *in vivo*[14].

The goals of this research were to use zebrafish as a model to: 1) characterize the spatial and temporal expression of *adnpa/b* during early embryonic development, 2) generate an *adnpa*$^{-/-}$ */adnpb*$^{-/-}$ mutant line using CRISPR/cas9, 3) study the functional role of *adnpa/b* using the mutant line, overexpression studies, and RNA-seq. This research was also done in collaboration with the Hoffman Lab at Yale School of Medicine with the goal of studying behavioral phenotypes associated with *adnpa/b* loss of function during larval development. Zebrafish larvae also lend themselves to high throughput drug screens due to their small size, the ease of animal husbandry, and the ability to dissolve water soluble compounds in the larvae's environment.

Recently, our lab published data on the optimization of CRISPR/cas13d for RNA knockdown of maternal and zygotic transcripts in zebrafish embryos[24]. Attempts to establish RNA interference technologies in zebrafish have largely failed, thus Cas13d technology presents a unique opportunity for developmental biologists as it is the first tool of its kind to efficiently and specifically degrade maternal components during the earliest stages of embryogenesis[24]. Experiments reported herein also detail preliminary data for cas13d knockdown of *adnpa/b* in zebrafish embryos as well as a method for improved knockdown efficiency using a modified sgRNA.

The diagnosis and treatment of ADNP syndrome faces a number of challenges, so novel model systems are needed to assess the nature of the developmental defects. Importantly, diagnosis is limited to the identification of relevant symptoms including ASD, ID, and early tooth eruption[25,26]. There are currently no pharmacological interventions that directly address the mechanisms by which *adnp* syndrome develops and progresses. Treatment options are limited to physical and behavioral therapies, as well as symptom management[26]. Given these obstacles, this research aims to lay the groundwork for the investigation of the molecular pathology of *adnp*

syndrome, improvements in understanding the impact of mutations on development and behavior, and long term, the development of treatment options for human patients through high throughput drug screenings conducted using the *adnpa/b* mutant line. Additionally, as ADNP represents a common mechanism for multiple ASD risk genes (impacts on transcriptional regulation/chromatin modification), studying ADNP may prove beneficial in furthering our categorical understanding of the genetics of ASD.

MATERIALS AND METHODS

Husbandry: All research was conducted following approval from the University of New Haven's Institutional Animal Care and Use Committee (IACUC). TU-AB zebrafish were maintained on a 14:10 light to dark cycle at 28 ˚C. Feedings were performed twice daily, and fish filter systems were monitored and maintained regularly.

Breeding: Pairs of zebrafish were bred in breeding tanks for each breeding session. Tanks of zebrafish were not bred more than once in a two-week period. Embryos were collected for either microinjection, controls, or to be raised for a new generation.

RNA Extraction: For each RNA extraction 20 zebrafish embryos were snap frozen using liquid nitrogen at the appropriate developmental stage. Trizol was used with chloroform to extract the RNA and the RNA was stored at -80 ˚C in nuclease free water.

cDNA Synthesis: The extracted RNA was used with Invitrogen's SuperScript™ III First-Strand Synthesis kit (cat. No. 18080-051) to perform RT-PCR. cDNA was stored at -20 ˚C in nuclease free water.

Microinjection: Embryos were harvested from TU-AB strain zebrafish. Embryos were dechorionated with Protease from *Streptomyces griseus* from Sigma (cat. No. P5147-5G). Embryos were loaded into gel-molds and needle contents were injected directly into the cell at the one cell stage. Cas9 mRNA was injected at a concentration of 100 ng/uL with 2-4 sgRNAs each at a final concentration of 80 ng/uL. For *adnpa/b* CRISPR/cas9 injections, sgRNAs targeting the *slc45a2* albino locus was used as a control for cas9. Cas13d mRNA was injected at a concentration of 300 ng/uL with 3 sgRNAs per gene at a final concentration of 200 ng/uL. For *adnpa/b* CRISPR/cas13d knockdown, the no-tail gene *tbxta* was used as a control.

Quantifying RNA Expression Levels: To determine the expression levels of the target genes, qPCR was performed on the cDNA extracted from the embryos used in the developmental timecourse and cas13d knockdown experiments. qPCR primers were designed for each experiment with *rpl13a* used as control (table 1). GeneCopoeia's All-in-One™ qPCR Mix (cat.No. QP001) was used along with the manufacturer protocol as well as the Bio-Rad's CFX96™ Touch Real-Time PCR Detection System. Quantification results were exported, and analysis was done in excel to calculate the fold changes for both *adnpa* and *adnpb*.

Genotyping: Genotyping was performed using single or pooled embryos ranging from 0-72 hpf, or rear fin clips from adult fish. All genotyping was performed in compliance with IACUC protocols. Since amplifying both the wildtype and truncated allele in a single PCR was unreliable given their size difference, a second pair of PCR primers was designed to selectively amplify the wildtype allele (table 1). This was accomplished by designing the primers to amplify the region of the coding sequence that was deleted in the truncation (figure 7A). Together these primer sets were utilized to distinguish between wildtype, heterozygous and homozygous mutants.

mRNA *In Vitro* Transcription: The coding sequence for *adnpa* was amplified using primers containing ClaI and XhoI site overhangs (table 1). The PCR amplicon was cloned into a PCS2 expression vector (figure 1) and *in vitro* transcribed using the MEGAscript SP6 Transcription Kit (Cat. No. AM1330).

***In Situ* Hybridization**: *In situ* hybridization was performed following the protocol outlined in Thisse et. al, 2008. Embryos were fixed in 4% paraformaldehyde at 24 hpf. Primers for RNA probes of *adnpa/b* were designed to bind the entire transcript to ensure any partial transcription in mutant alleles would be captured (table 1).

RESULTS

Adnpa/b Expression Over the First 48 hours of Development Post Fertilization

Three biological replicates of 20 dechorionated embryos were sacrificed in accordance with IACUC procedures at 0, 2.5,6,12,24, and 48 hours post fertilization (hpf). Following RNA extraction and cDNA synthesis, qPCR was performed to amplify *adnpa, adnpb,* and *rpl13a.* Three technical replicates were performed for each of the three biological replicates. ΔCt values for *adnpa/b* were calculated by normalizing to *rpl13a* and relative expression was determined by normalizing to the 0 hpf timepoint for each paralog (figure 2). *adnpa/b* are both maternally inherited and strongly expressed, with expression increasing dramatically following zygotic genome activation at 2 – 2.5 hpf and then decreasing rapidly by the 6 hour time point. Expression continues to decrease to the 12 hpf timepoint. *adnpa* remains relatively consistent out to 48 hpf. *adnpb* increases slightly at 24 hpf and then decreases again out to 48 hpf.

In Situ Hybridization for *adnpa/b* at 24 Hours Post Fertilization

TUAB wildtype fish were crossed, and embryos were collected and raised to 24 hpf at 28^{o}C. Embryos were then manually dechorionated with tweezers and sacrificed, then fixed in 4% paraformaldehyde. Whole mount *in situ* hybridization was performed following Thisse et. al, 2008. Both *adnpa/b* show similar patterns with expression being restricted to the anterior structures, with strong expression in the brain and eyes (figure 3).

Strategy for Generating Loss of Function by Transcriptless and Null Alleles for *adnpa* and *adnpb*

Given the potential dominant negative effect observed in humans with ADNP syndrome, as well as recent reports of genetic compensation in zebrafish genes with multiple paralogs, a CRISPR/Cas9 knockout strategy was designed to specifically avoid these pitfalls[27]. For *adnpa*, sgRNAs were design to target 1) upstream from the core promoter and 2) in the last exon, exon 4(figure 4). Given the heterogeneity observed in sequences outside of coding regions, the *adnpa* promoter of 4 fish was sequenced and a sgRNA was designed based off a sequence conserved among all 4 fish. These fish (2 male and 2 female) were used to generate the embryos that were injected with *adnpa* sgRNAs + Cas9 mRNA. Through the coinjection of these two guides, a 2.5 kb deletion could be generated, which would result in loss of the core promoter, transcription start, 5' UTR, start codon, and a large region of the coding sequence. The resulting allele should completely lack transcription, and thus lack any downstream compensatory mechanism, or translation of aberrant protein.

For *adnpb*, a similar strategy was initially adopted, however following Sanger Sequencing, only a 6 bp, in frame deletion, was observed at the site of the exon 4 sgRNA. This 6

bp deletion was consistently generated from one experiment to the next. Additionally, the noncoding exons 1 and 2 in *adnpb*, are separated by an 11 kb intron. The larger size separation between promoter and exon guides, may have also impacted the repair processes and thus the frequency with which a large deletion would be generated.

To combat this, a new strategy was adopted for *adnpb.* 4 sgRNAs were designed spanning exon 4, beginning with sgRNA 1 at the beginning of exon 4, not far downstream from the start codon in the small exon 3 (figure 4). Through the coinjection of 4 sgRNAs targeting exon 4, a 2kb deletion could be generated, near the start codon. Should this deletion result in a truncation and frameshift, the resulting protein product would be non-functional. Additionally, because exon 4 is the last exon, a frameshift generated here would likely avoid triggering genetic compensation via the nonsense mediated decay pathway[27].

Genotyping Strategy for *adnpa/b*

PCR primers were designed flanking sgRNAs 1 / 2 for *adnpa* and flanking sgRNAs 1 / 4 for *adnpb* (figure 5A). PCR amplification of *adnpa* would result in a 3kb amplicon for wildtype alleles and a 500 bp amplicon for the truncated allele. For *adnpb*, PCR amplification would result in a 2kb amplicon for wildtype and a 500 bp amplicon for the truncated allele. Following PCR genotyping and gel electrophoresis, a 500 bp band was observed for *adnpa* (figure 5B). Sanger Sequencing of this band confirmed that there was a 2.5kb deletion spanning sgRNA 1 and 2 in *adnpa* (figure 5A). Following genotyping and gel electrophoresis for *adnpb*, two ~800 bp bands were observed (figure 5B). Sanger Sequencing of these bands confirmed there were two different alleles within mosaic F0s, one spanning sgRNAs 1-3 and one spanning sgRNAs 2-4. Both resulted in ~1.2 kb deletions as well as frameshifts (figure 5A). Allele 1(sgRNAs 1-3)

had a stop codon two codons downstream from the truncation, resulting in a loss of all but the first 144/1003 amino acids. Based on the protein domain prediction software InterProScan, with the exception of two zinc finger domains, all of the predicted domains, including the homeobox domain, are lost due to truncation. Additionally, the conserved neuroprotective peptide sequence ISPQ(360-363) commonly referred to as NAP(NAPVISPQ) is no longer present (figure 5C).

F1 fish with allele 1 were crossed to generate a stable heterozygous line for *adnpb* truncation. The same was done for the *adnpa* truncation. *Adnpa*$^{-/-}$ and *adnpb*$^{+/-}$ fish were crossed to generate putative *adnpa*$^{+/-}$*b*$^{+/-}$ embryos. These embryos were raised to adulthood and screened by fin clip PCR genotyping for *adnpb* truncation (figure 6). Small sections of the ends of Zebrafish rear fins can be surgically removed without permanent damage to the organism, as Zebrafish rear fins have an incredible regenerative capability and will fully heal in approximately 2 weeks' time. Since these fish were the offspring of an *adnpa* $^{-/-}$ mother, all fish of this generation were expected to have *adnpa* truncations (figure 6). PCR genotyping of *adnpa* and *adnpb* showed genotypes consistent with the expected mendelian ratios (100% heterozygous *adnpa* truncation, 50% heterozygous *adnpb* truncation).

Genotyping Strategy for Distinguishing between Wildtype, Heterozygous and Homozygous Alleles

Due to the large difference in amplicon size, wildtype and truncated PCR amplicons could not be reliably amplified together within a single PCR reaction. To consistently and reliably distinguish between wildtype, heterozygous and homozygous mutant alleles, a second set of PCR primers were designed which would amplify a region of the coding sequence that was expected to be deleted in the truncated allele (figure 7A). Thus, through the combination of two PCR reactions, one which would amplify only the wildtype product, and one which amplified the

truncated product, wildtype, heterozygous and homozygous mutants could be reliably distinguished (figure 7B/7C).

adnpa Truncation from promoter to exon 4 leads to total loss of transcription

To determine whether the strategy for generation of an *adnpa* transcriptless allele was successful, whole mount *in situ* hybridization (WMISH) was performed on 24 hpf embryos collected following intercross of *adnpa*$^{+/-}$ fish. WMISH was performed following the protocol from Thisse et al., 2008 using 30 ng of *adnpa* DIG-labelled RNA probe. Following staining and visualization, embryos clearly fell into one of 3 classes of staining intensity: no staining, light staining, or dark staining (identical to wildtype control embryos). Stained embryos were sorted and counted. Incredibly, the staining intensity was consistent with mendelian ratios expected for homozygous, heterozygous and wildtype embryos (figure 8). DNA was extracted from single embryos of each staining class and PCR genotyping was performed to amplify both the wildtype and truncated alleles. Gel electrophoresis and imaging revealed that the genotype of the no-staining embryos was in fact homozygous mutant, the light staining heterozygous, and the dark staining, wildtype. This demonstrates that the transcriptless allele CRISPR/Cas9 knockout strategy fully ablated *adnpa* expression.

Phenotype Analysis of *adnpa* $^{-/-}$ / *b* $^{-/-}$ Embryos During the First 7 Days Post Fertilization

3 pairs of double heterozygous fish were intercrossed to generate putative *adnpa/b* double homozygous mutants. Embryos were monitored over the first 7 days post fertilization. Despite WMISH data showing expression in the brain and eyes of the embryo, no obvious morphological changes were observed in offspring of the double heterozygous intercrosses (figure 9).

Adnpa mRNA Overexpression in Wildtype Embryos

100 embryos were injected at a one cell stage with 50,100, and 150 pg of *adnpa* or GFP (control) mRNA. No obvious morphological changes were observed over the first 72 hours post fertilization in the 50 and 100 pg injections (figure 10). At 150 pg, both *adnpa* and GFP mRNA injections showed severe and nonspecific developmental defects suggesting these changes were due to toxicities associated with high mRNA concentrations.

CRISPR/Cas13d Knockdown of *adnpa*

Given the high maternal and early zygotic expression observed in the timecourse qPCR data, there may be a critical role for *adnpa/b* during the early stages of embryogenesis. Following our recent optimization of cas13d for RNA knockdown in zebrafish, cas13d sgRNAs were designed for knockdown of *adnpa* and *adnpb* (figure 11b). Following coinjection of cas13d mRNA and 3 *adnpa* sgRNAs, embryos were observed and raised to 72 hpf. No obvious phenotype was observed during this time period. Given the lack of phenotype, qPCR was performed to assess the knockdown efficiency. Following injection, embryos were raised to 6hpf, RNA was extracted, and cDNA was synthesized. 6 hpf was selected for its relatively high expression level of *adnpa*, while also providing ample time for cas13d translation, guide RNA complexing and RNA degradation to occur. qPCR was performed for *adnpa* and housekeeping gene *rpl13a*. An average 51% knockdown efficiency was observed for *adnpa* (figure 12).

CRISPR/Cas13d Knockdown Efficiency is Improved by Disruption of a Stem-Loop Structure in Cas13d gRNAs

In addition to the *adnpa* sgRNAs previously injected, a second injection group was performed. The sgRNAs used in this group, were prepared using a universal primer with an A →T substitution at the 5' end of the primer. Our colleague, Dr. Miguel A. Moreno-Mateos at the Andalusian Center for Developmental Biology has suggested that this position within the sgRNA may facilitate the formation of a stem-loop structure. Dr. Moreno-Mateos has hypothesized that disruption of this stem loop structure may improve knockdown efficiency of the Cas13d system (data unpublished). In fact, a 7% average increase in knockdown efficiency was observed, between the original universal primer *adnpa* sgRNAs, and the stem loop disruption universal primer *adnpa* sgRNAs (figure 12).

DISCUSSION

Genome wide association studies have identified hundreds of polymorphisms associated with autism spectrum disorders. Among them, *ADNP* has been shown to be one of the most prevalent autism risk genes[28–30]. *ADNP* mutation not only causes the severe developmental disorder, ADNP syndrome, but is also associated with the progression of Alzheimer's disease and neuropsychiatric disorders like schizophrenia[1,11,12]. *Adnp*'s clear neurodevelopmental and neuroprotective roles are well supported in the literature; with numerous studies highlighting the effects of *adnp* mutation and NAP peptide rescue on neuronal apoptosis and survival signalling[11,16-18]. Additionally, mouse models of *adnp* loss of function have demonstrated that *adnp* is required for brain development, as homozygous mice are embryonic lethal due to cranial neural tube failure and death at E8.5-9.0. Studies on heterozygous mice were also shown to have

intellectual disabilities, which could be rescued by NAP peptide administration[13,17,19]. While progress has been made in understanding the effects of *adnp* on neurodevelopment, the molecular mechanisms by which *adnp* regulates developmental processes remain poorly understood. Additionally, given the high prevalence of social and behavioural deficits observed in ASD, more research is needed to understand how *adnp* impacts higher cognitive functions. Our colleagues in the Hoffman Lab at Yale School of Medicine have pioneered a high throughput system for studying behavioural deficits in zebrafish, including parameters such as rest/wake activity, and seizure susceptibility[31]. Additionally, the rapid generation times and highly homologous genomes of zebrafish make them an excellent model for studying human genetic disorders. Their aquatic nature also allows for rapid screening of water-soluble drugs. Thus, in this study zebrafish were chosen as a model system for *adnp* loss of function.

The spatial and temporal expression of *adnp* was characterized during zebrafish embryonic development through qPCR and whole mount *in situ* hybridization. The two *adnp* paralogs in zebrafish, *adnpa* and *adnpb* are both maternally expressed, and following zygotic genome activation, increase in expression by 2.5 hpf. Expression then rapidly decreased by the 6 and 12 hpf timepoint. While *adnpa* remains relatively constant throughout the rest of the 48 hpf, *adnpb* appears to spike at 24 hpf, then decrease by the 48 hpf timepoint. WMISH data shows that at 24 hpf, *adnpa/b* expression is localized to the anterior of the embryo, with strong expression in the developing brain and eyes. This observation is in agreement with work done in mouse and cell culture models, highlighting the neurodevelopmental role of *adnp.* Future experiments will aim to characterize the expression further by examining later time points through both qPCR and WMISH.

It should be noted that the housekeeping gene, *rpl13a,* which was used in qPCR normalization, is a constitutively expressed ribosomal protein. Following observations from WMISH, which show that *adnpa/b* are localized to the anterior, it is now clear that while all cells from which RNA was extracted contain *rpl13a,* not all cells were expressing *adnpa/b.* Thus, the ratio of *rpl13a* to *adnpa/b* changes over the course of development. It may be that the degree to which *adnpa/b* expression decreases by the 24 hpf timepoint is exaggerated.

In order to study the effect of *adnpa/b* loss of function on embryonic development, a strategy was developed for *adnpa* knockout which would result in a transcriptless allele. Through the generation of a large deletion spanning the promoter to exon 4, the core promoter, transcription start, 5' UTR, start codon, and a portion of the coding sequence were deleted. Additionally, a frameshift was generated downstream of the truncation. The ablation of *adnpa* expression was confirmed by WMISH, by demonstrating that homozygous mutants completely lack staining of a DIG-labelled *adnpa* RNA probe. There were several challenges previously highlighted when repeating the transcriptless allele strategy with *adnpb.* Thus, a new strategy was adopted in which 4 sgRNAs spanning exon 4, would generate a large deletion in the coding sequence. The resulting truncation and frameshift, lead to a loss of all but the first 144/1003 amino acids. Consistent with the human homolog *adnp,* the protein domain prediction software InterProScan, identified several conserved C2H2 zinc finger domains, and a homeobox domain, in *adnpb.* All but the first two zinc finger domains were lost in the truncated allele. Additionally, the neuroprotective peptide ISPQ(NAPVISPQ) was lost due to truncation. Based off of this, it is expected that the *adnpb* truncation should result in loss of function. Additionally, with the truncation occurring in exon 4, the last exon, genetic compensation via the nonsense mediated decay pathway should be avoided. Future experiments may include injection of Ha-tagged

wildtype and truncated *adnpb* mRNA to determine if the truncated protein product is stable or degraded after translation. Additionally, qPCR of heterozygous and homozygous *adnpb* mutants can be utilized to identify any subtle changes in transcript expression not identified by WMISH.

Stable heterozygous *adnpa* and *adnpb* lines as well as a double heterozygous line have now been established. While no gross morphological deficits were observed in double homozygous mutants, the offspring of the double heterozygous intercross are being raised to evaluate whether double homozygotes are viable. Double heterozygous fish will also be crossed with a dlx5a/6a, vglut reporter line. This transgenic line co-labels GABAergic and glutamatergic neurons, which the Hoffman lab has used to study another autism-risk gene mutant, *cntnap2*, which they identified as having regional GABAergic deficits [31]. Another zebrafish autism risk gene mutant, *grin1a* was recently shown to impact the midline crossing of axons from glutamatergic neurons[21]. *Grin1a* is a subunit of the NMDA receptor, which is upstream of *adnp* activation in excitatory glutamatergic synapse[32]. While there is no obvious morphological change in the *adnpa/b* double homozygous mutant, there may be a more subtle phenotype which becomes apparent following crossing to one or more neurological reporter lines.

Despite the covid-19 pandemic, this research continued largely uninterrupted, with the exception of the initial shutdown in the Spring of 2020. This shutdown period delayed the generation of the mutant lines substantially, and thus the behavioural assays with our collaborators at the Hoffman Lab, and the RNA-seq experiments were delayed. In addition to the reporter line crossings, these experiments will prove critical in uncovering how *adnp* loss of functions impacts development. The Hoffman lab has demonstrated that the zebrafish behavioural assays can be utilized for high throughput screening of chemical matter, to identify drugs which modify, or reverse observed behavioural deficits[31]. Should a behavioural phenotype

be identified in the *adnp*a/*b* mutant, these drug screenings could be performed, to identify potential treatments for *adnp* syndrome.

Cas13d optimization in zebrafish has opened the door for studying the role of maternally deposited mRNAs during early embryogenesis. Given the maternal expression observed in the qPCR data, there may be an early role for maternally deposited *adnpa/b*. While no phenotype was observed in the *adnpa* knockdown experiment, this may be due to compensation by *adnpb*. It may also be that the knockdown efficiency was insufficient for a phenotype to develop. In a recent publication, an average 70% knockdown was reported for cas13d in zebrafish[24]. Even with the improved stem loop disruption universal primer, an average 58% knockdown was observed across biological and technical triplicates for *adnpa* knockdown. *Adnpa/b* sgRNAs have been redesigned to attempt to improve the efficiency of knockdown, however the degree of knockdown which is sufficient for the development of a phenotype is unknown. Lastly, as is the case in the homozygous double knockout line, there may be a phenotype in the cas13d knockdown that is too subtle to be identified by simple light microscopy. Future experiments that aim to identify key differences in neuronal development in the mutant line, may prove useful in studying the effects of Cas13d-mediate knockdown.

REFERENCES

1. Helsmoortel C, Vulto-Van Silfhout AT, Coe BP, et al. A SWI/SNF-related autism syndrome caused by de novo mutations in ADNP. *Nat Genet*. 2014;46(4):380-384. doi:10.1038/ng.2899
2. Lam KSL, Aman MG. The Repetitive Behavior Scale-Revised: Independent Validation in Individuals with Autism Spectrum Disorders. *J Autism Dev Disord*. 2007;37(5):855-866. doi:10.1007/s10803-006-0213-z
3. Baio J, Wiggins L, Christensen DL, et al. Prevalence of Autism Spectrum Disorder Among Children Aged 8 Years — Autism and Developmental Disabilities Monitoring Network, 11 Sites, United States, 2014. *MMWR Surveill Summ*. 2018;67(6):1-23. doi:10.15585/mmwr.ss6706a1
4. Schaaf CP, Zoghbi HY. Solving the Autism Puzzle a Few Pieces at a Time. *Neuron*. 2011;70(5):806-808. doi:10.1016/j.neuron.2011.05.025
5. Pinto D, Delaby E, Merico D, et al. Convergence of Genes and Cellular Pathways Dysregulated in Autism Spectrum Disorders. *Am J Hum Genet*. 2014;94(5):677-694. doi:10.1016/j.ajhg.2014.03.018
6. Iakoucheva LM, Muotri AR, Sebat J. Getting to the Cores of Autism. *Cell*. 2019;178(6):1287-1298. doi:10.1016/j.cell.2019.07.037
7. Krumm N, O'Roak BJ, Shendure J, Eichler EE. A de novo convergence of autism genetics and molecular neuroscience. *Trends Neurosci*. 2014;37(2):95-105. doi:10.1016/j.tins.2013.11.005
8. Vandeweyer G, Helsmoortel C, Van Dijck A, et al. The transcriptional regulator *ADNP* links the BAF (SWI/SNF) complexes with autism. *Am J Med Genet Part C Semin Med*

Genet. 2014;166(3):315-326. doi:10.1002/ajmg.c.31413

9. Krajewska-Walasek M, Jurkiewicz D, Piekutowska-Abramczuk D, et al. Additional data on the clinical phenotype of Helsmoortel-Van der Aa syndrome associated with a novel truncating mutation in *ADNP* gene. *Am J Med Genet Part A*. 2016;170(6):1647-1650. doi:10.1002/ajmg.a.37641
10. Satterstrom FK, Kosmicki JA, Wang J, et al. Novel genes for autism implicate both excitatory and inhibitory cell lineages in risk. *bioRxiv*. Published online December 1, 2018:484113. doi:10.1101/484113
11. Gozes I, Divinski I. NAP, A Neuroprotective Drug Candidate in Clinical Trials, Stimulates Microtubule Assembly in the Living Cell. *Curr Alzheimer Res*. 2007;4(5):507-509. doi:10.2174/156720507783018208
12. Dresner E, Agam G, Gozes I. Activity-dependent neuroprotective protein (ADNP) expression level is correlated with the expression of the sister protein ADNP2: Deregulation in schizophrenia. *Eur Neuropsychopharmacol*. 2011;21(5):355-361. doi:10.1016/j.euroneuro.2010.06.004
13. Mandel S, Rechavi G, Gozes I. Activity-dependent neuroprotective protein (ADNP) differentially interacts with chromatin to regulate genes essential for embryogenesis. *Dev Biol*. 2007;303(2):814-824. doi:10.1016/j.ydbio.2006.11.039
14. Dresner E, Malishkevich A, Arviv C, et al. Novel Evolutionary-conserved Role for the Activity-dependent Neuroprotective Protein (ADNP) Family That Is Important for Erythropoiesis. *J Biol Chem*. 2012;287(48):40173-40185. doi:10.1074/jbc.M112.387027
15. Mandel S, Rechavi G, Gozes I. Activity-dependent neuroprotective protein (ADNP) differentially interacts with chromatin to regulate genes essential for embryogenesis. *Dev*

Biol. 2007;303(2):814-824. doi:10.1016/j.ydbio.2006.11.039

16. Giladi E, Hill JM, Dresner E, Stack CM, Gozes I. Vasoactive Intestinal Peptide (VIP) Regulates Activity-Dependent Neuroprotective Protein (ADNP) Expression In Vivo. *J Mol Neurosci*. 2007;33(3):278-283. doi:10.1007/s12031-007-9003-0
17. Vulih-Shultzman I, Pinhasov A, Mandel S, et al. Activity-dependent neuroprotective protein snippet NAP reduces tau hyperphosphorylation and enhances learning in a novel transgenic mouse model. *J Pharmacol Exp Ther*. 2007;323(2):438-449. doi:10.1124/jpet.107.129551
18. Zamostiano R, Pinhasov A, Gelber E, et al. Cloning and characterization of the human activity-dependent neuroprotective protein. *J Biol Chem*. 2001;276(1):708-714. doi:10.1074/jbc.M007416200
19. Pinhasov A, Mandel S, Torchinsky A, et al. Activity-dependent neuroprotective protein: a novel gene essential for brain formation. *Brain Res Dev Brain Res*. 2003;144(1):83-90. Accessed May 6, 2019. http://www.ncbi.nlm.nih.gov/pubmed/12888219
20. Krumm N, Turner TN, Baker C, et al. Excess of rare, inherited truncating mutations in autism. *Nat Genet*. 2015;47(6):582-588. doi:10.1038/ng.3303
21. Gao J, Stevenson TJ, Douglass AD, Barrios JP, Bonkowsky JL. The midline axon crossing decision is regulated through an activity-dependent mechanism by the NMDA receptor. *eNeuro*. 2018;5(2). doi:10.1523/ENEURO.0389-17.2018
22. Dooley K, Zon LI. Zebrafish: a model system for the study of human disease. *Curr Opin Genet Dev*. 2000;10(3):252-256. doi:10.1016/S0959-437X(00)00074-5
23. Howe K, Clark MD, Torroja CF, et al. The zebrafish reference genome sequence and its relationship to the human genome. *Nature*. 2013;496(7446):498-503.

doi:10.1038/nature12111

24. Kushawah G, Hernandez-Huertas L, Abugattas-Nuñez del Prado J, et al. CRISPR-Cas13d Induces Efficient mRNA Knockdown in Animal Embryos. *Dev Cell*. Published online August 7, 2020. doi:10.1016/j.devcel.2020.07.013
25. Gozes I, Van Dijck A, Hacohen-Kleiman G, et al. Premature primary tooth eruption in cognitive/motor-delayed ADNP-mutated children. *Transl Psychiatry*. 2017;7(2). doi:10.1038/tp.2017.27
26. Gozes I. The ADNP Syndrome and CP201 (NAP) Potential and Hope. *Front Neurol*. 2020;11:608444. doi:10.3389/fneur.2020.608444
27. El-Brolosy MA, Kontarakis Z, Rossi A, et al. Genetic compensation triggered by mutant mRNA degradation. *Nature*. 2019;568(7751):193-197. doi:10.1038/s41586-019-1064-z
28. Feliciano P, Zhou X, Astrovskaya I, et al. Exome sequencing of 457 autism families recruited online provides evidence for autism risk genes. *npj Genomic Med*. 2019;4(1):1-14. doi:10.1038/s41525-019-0093-8
29. Rossi M, El-Khechen D, Black MH, Farwell Hagman KD, Tang S, Powis Z. Outcomes of Diagnostic Exome Sequencing in Patients With Diagnosed or Suspected Autism Spectrum Disorders. *Pediatr Neurol*. 2017;70:34-43.e2. doi:10.1016/j.pediatrneurol.2017.01.033
30. Satterstrom FK, Kosmicki JA, Wang J, et al. Large-Scale Exome Sequencing Study Implicates Both Developmental and Functional Changes in the Neurobiology of Autism. *Cell*. 2020;180(3):568-584.e23. doi:10.1016/j.cell.2019.12.036
31. Hoffman EJ, Turner KJ, Fernandez JM, et al. Estrogens Suppress a Behavioral Phenotype in Zebrafish Mutants of the Autism Risk Gene, CNTNAP2. *Neuron*. 2016;89(4):725-733. doi:10.1016/j.neuron.2015.12.039

32. Sragovich S, Malishkevich A, Piontkewitz Y, et al. The autism/neuroprotection-linked ADNP/NAP regulate the excitatory glutamatergic synapse. *Transl Psychiatry*. 2019;9(1):1-14. doi:10.1038/s41398-018-0357-6

FIGURES

TABLE 1: PCR primers designed for genotyping, ISH probes, mRNA overexpression, and qPCR.

Name	Sequence (5' to 3')	Direction	Notes
AdnpaF2	GCTATAGCCCGCTTGACTGG	Forward	Genotyping: Amplifies wildtype(3kb) and truncated(0.5kb) adnpa
AdnpaR1	TGCTGCACCAGTGCTTCATA	Reverse	
AdnpB_F_new	CTGAACTGCCCCTATTGCAC	Forward	Genotyping: Amplifies wildtype(2kb) and truncated(0.7kb) adnpb
AdnpB_R_new	CGATTTGAGAAGTGGCTCGC	Reverse	
Adnpa probe fwd	GCAAGTGTCTGTACTGTAACCG	Forward	ISH: For creating antisense DIG-lab RNA probe
Adnpa probe rev	TAATACGACTCACTATAGGGGTAAAG TCCCGGTCACATAAGC	Reverse	ISH: Contains T7 site (TAATACGACTCACTATAGGG)
Adnpb probe fwd	CTAGTAACATGACGGCTTCCAC	Forward	ISH: For creating antisense DIG-lab RNA probe
Adnpb probe rev	TAATACGACTCACTATAGGGCATCAG AGTCACTCCCTTCAAC	Reverse	ISH: Contains T7 site (TAATACGACTCACTATAGGG)
Adnpa_ClaI_F	CGCGATCGATGAGATGTTTCAGCTTC CAGTG	Forward	For Cloning into PCS2: Contains ClaI Restriction Site
Adnpa_XhoI_R	GCGCCTCGAGTCATCTACCAAGCAAC CC	Reverse	For Cloning into PCS2: Contains XhoI Restriction Site
Adnpa_wtonly_F	TGGGCTGGTATCTGGAACAG	Forward	Genotyping: Only amplifies wildtype adnpa allele
adnpa_wtonly_R	CCTTGAAGGGCTTGGTTTTC	Reverse	
adnpb_wtonly_F	TTTGAAACCAGGGGCTACAC	Forward	Genotyping: Only amplifies wildtype adnpb allele
adnpb_wtonly_R	ACTGCTGAAACCTTTTCTGC	Reverse	
ADNPA_F_qPCR	TCAGCCAATGCTCTGAACAC	Forward	qPCR primers
ADNPA_R_qPCR	TTCGGGGAATAGTTCATTGC	Reverse	
adnpb-forward	GCCCTTTTTCACACGCCATT	Forward	qPCR primers
adnpb-reverse	CGTTTGCGATGATGCACAGT	Reverse	
rpl13a_qPCR_f	TAAGGACGGAGTGAACAACCA	Forward	qPCR primers
rpl13a_qPCR_r	CTTACGTCTGCGGATCTTTCTG	Reverse	
adnpa_sgRNA_In	TAATACGACTCACTATAGGGTAGCCT ATACGAAAGGGTTTTAGAGCTAGAA	Reverse	sgRNAs for adnpa knockout
adnpa_sgRNA_E4	TAATACGACTCACTATAGGGTGATCG AAAGGAGCTCCGTTTTAGAGCTAGAA	Reverse	sgRNAs for adnpa knockout
adnpa_E4_g1	TAATACGACTCACTATAGGGTGTCAC TAGGTAGGTAAGTTTTAGAGCTAGAA	Reverse	sgRNAs for adnpb knockout
adnpb_E4_g4	TAATACGACTCACTATAGGTTTAGGT GAACCCCTGACGTTTTAGAGCTAGAA	Reverse	sgRNAs for adnpb knockout
adnpb_E4_g5	TAATACGACTCACTATAGGTTTCCCTG CTGAAGTGTAGTTTTAGAGCTAGAA	Reverse	sgRNAs for adnpb knockout
adnpb_E4_g6	TAATACGACTCACTATAGGGGGTATC TTTGGGATTGTGTTTTAGAGCTAGAA	Reverse	sgRNAs for adnpb knockout
Cas9Universal	AAAAGCACGACTCGGTGCCACTTTTT CAAGTTGATAACGGACTAGCCTTATT TTAACTTGCTATTTCTAGCTCTAAAAC	Forward	Used for Template Extension in Cas9 sgRNA Synthesis
13D-Universal	TAATACGACTCACTATAGGAACCCCT ACCAACTGGTCGGGGTTTGAAAC	Forward	Used for Template Extension in Cas13d sgRNA Synthesis
sId_13D-Universal	TAATACGACTCACTATAGGTACCCCT ACCAACTGGTCGGGGTTTGAAAC	Forward	Stem Loop Disruption Universal Primer Used for Template Extension in Cas13d sgRNA Synthesis

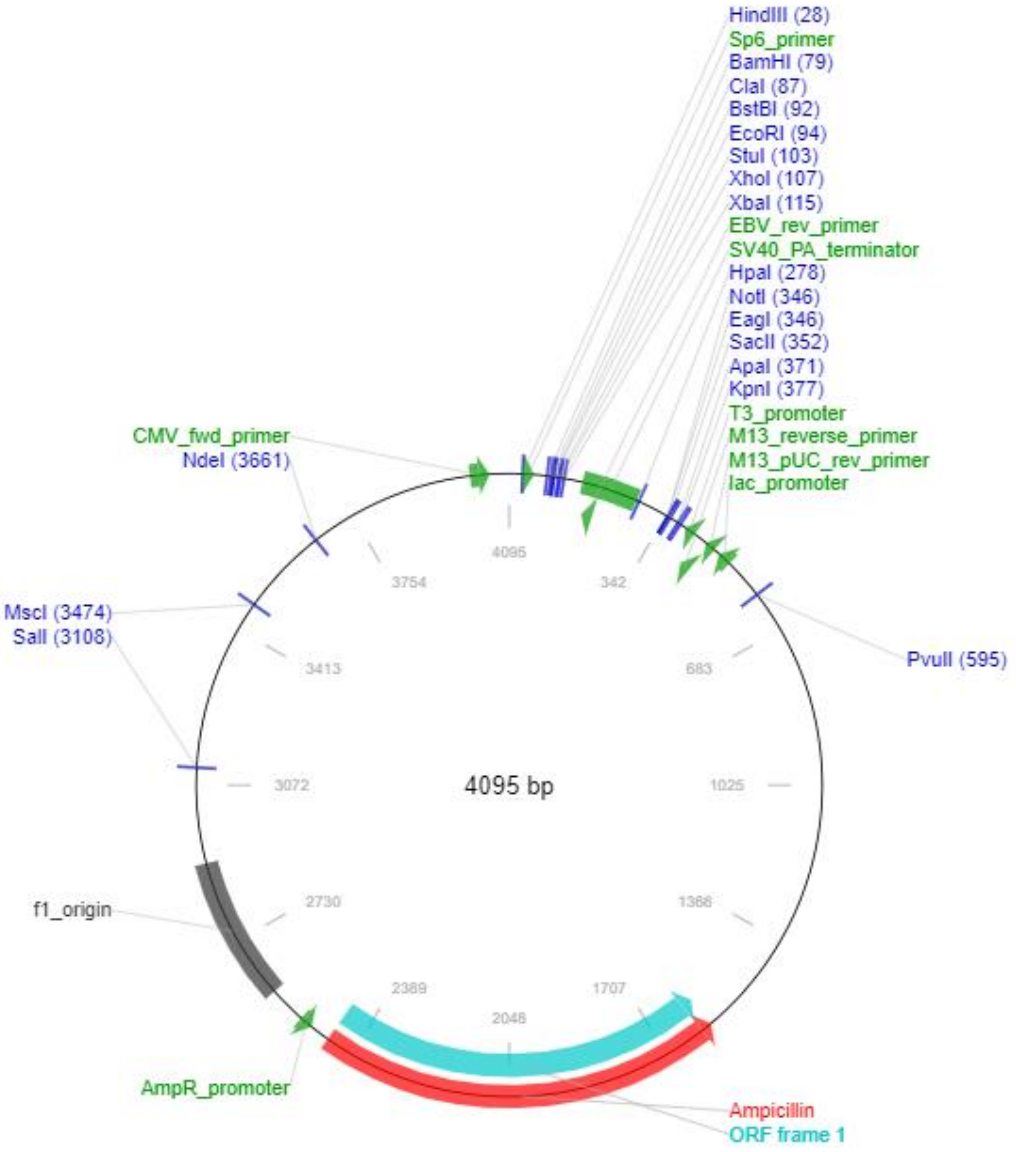

FIGURE 1: Map of the PCS2 plasmid used for *in vitro* transcription of *adnpa* mRNA. Coding sequence was cloned using ClaI and XhoI restriction sites.

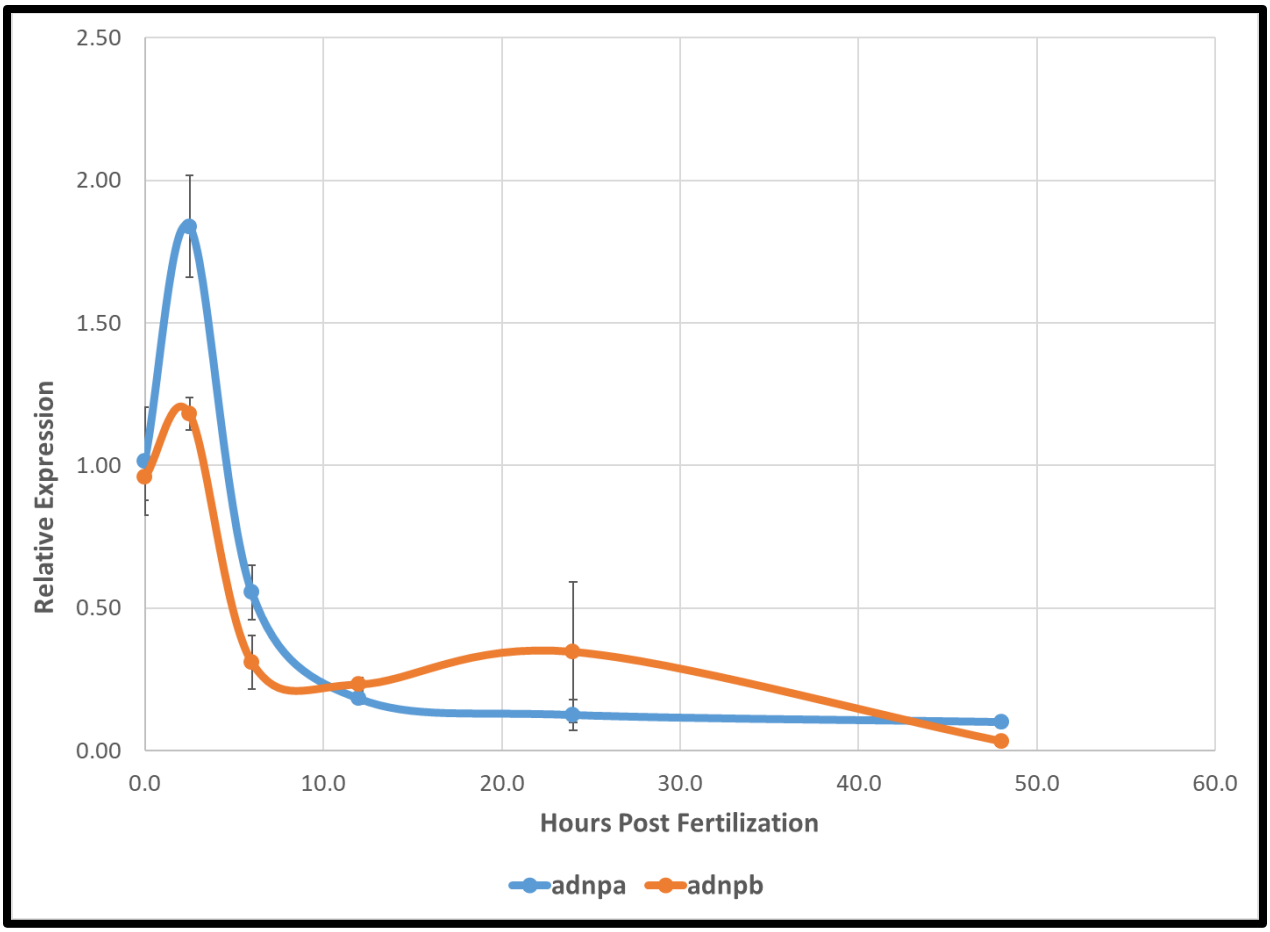

Figure 2: *adnpa/b* qPCR expression levels in wildtype embryos from 0-48 hours post fertilization. The ΔCt values were calculated using *rpl13a* levels as the house keeping gene. The relative expression shown above is normalized to the 0 hour time point for each of the two paralogs. Results represent both biological and technical triplicates.

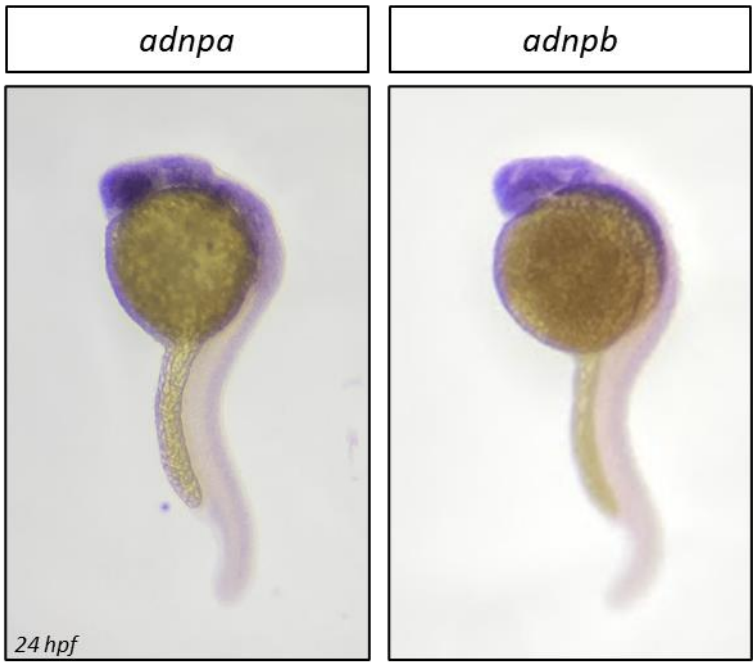

Figure 3: Representative images of whole mount *in situ* hybridization for *adnpa* and *adnpb* at 24 hours post fertilization. 30 ng of DIG-labeled RNA probe was used for labelling.

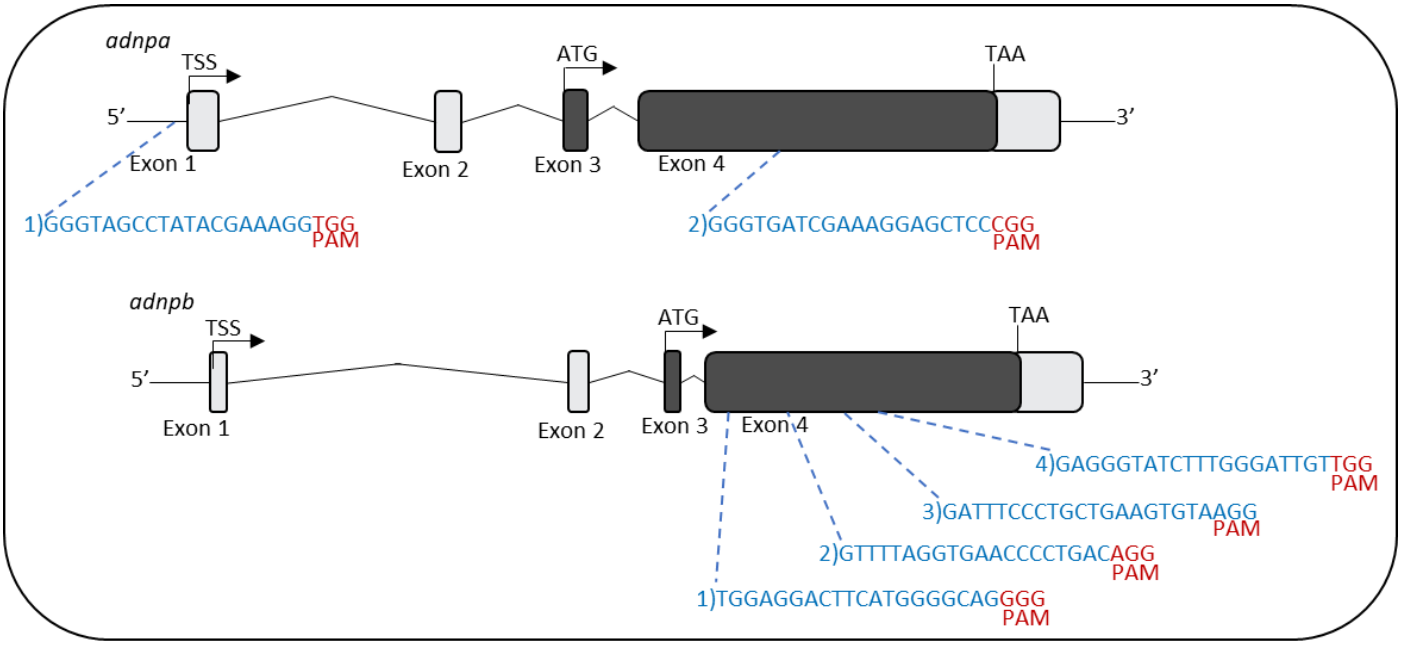

Figure 4: Strategy for Generating Null Alleles for *adnpa/b* using CRISPR/Cas9. Two sgRNAS, one targeting the promoter and one targeting exon 4, were used to generate a 2.5 kb deletion in *adnpa* resulting in a transcriptless allele. This truncation leads to a loss of the promoter, transcription start, 5' UTR, and start codon. Four sgRNAs spanning exon 4 were used to generate a 2 kb deletion. Beginning near the start of the coding sequence and generating a large deletion and frameshift, the resulting truncation should be a null.

A

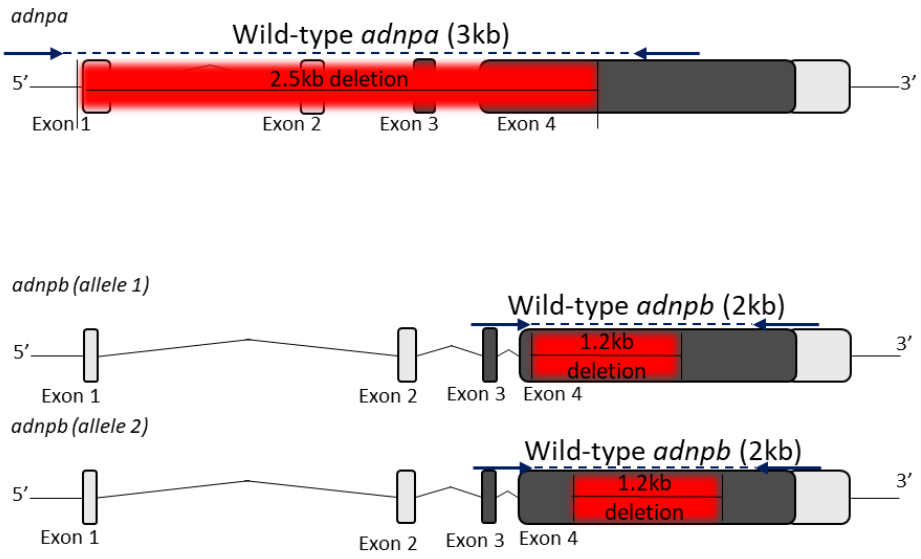
adnpa
Wild-type adnpa (3kb)
5'
2.5kb deletion
3'
Exon 1
Exon 2
Exon 3
Exon 4
adnpb (allele 1)
Wild-type adnpb (2kb)
5'
1.2kb deletion
3'
Exon 1
Exon 2
Exon 3
Exon 4
adnpb (allele 2)
Wild-type adnpb (2kb)
5'
1.2kb deletion
3'
Exon 1
Exon 2
Exon 3
Exon 4

B

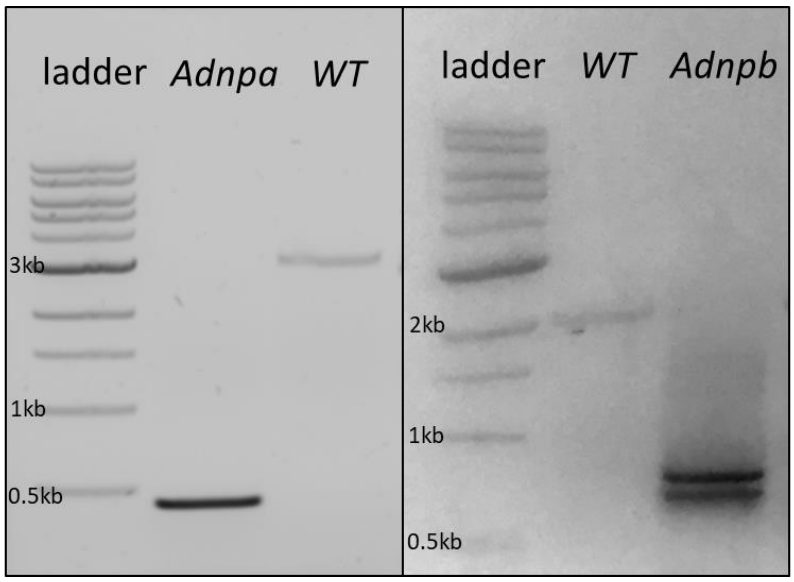
ladder
Adnpa
WT
3kb
1kb
0.5kb
ladder
WT
Adnpb
2kb
1kb
0.5kb

C

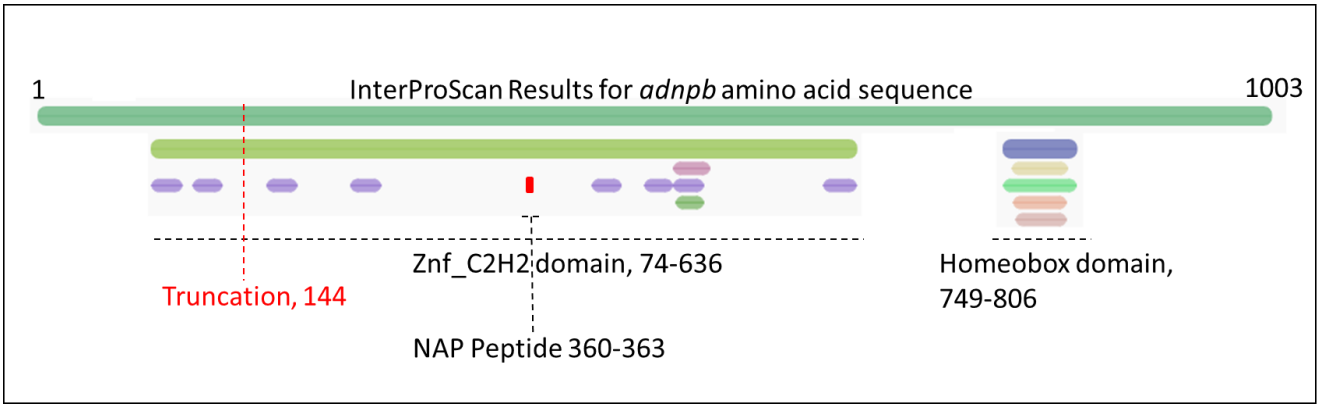
1
InterProScan Results for adnpb amino acid sequence
1003
Znf_C2H2 domain, 74-636
Homeobox domain, 749-806
Truncation, 144
NAP Peptide 360-363

Figure 5: A) Genotyping strategy and resulting Sanger Sequencing results for F0 embryo genotyping. Blue arrows represent forward and reverse primers. *Adnpa* genotyping resulted in a 2.5 kb deletion as expected based on sgRNA design. *Adnpb* genotyping resulted in two alleles within a pool of embryos, one spanning sgRNAs 1-3 and one spanning sgRNAs 2-4. Both resulted in a truncation and frameshift as confirmed by Sanger Sequencing. **B)** Representative gel image from PCR genotyping strategy for *adnpa/b* in F0 embryos. **C)** Graphical representation of the predicted protein domains for *adnpb* using InterProScan domain prediction software. With the exception of the first two zinc finger C2H2 domains, the rest of the zinc finger domains, NAP peptide, and homeobox domain are lost due to truncation in allele 1.

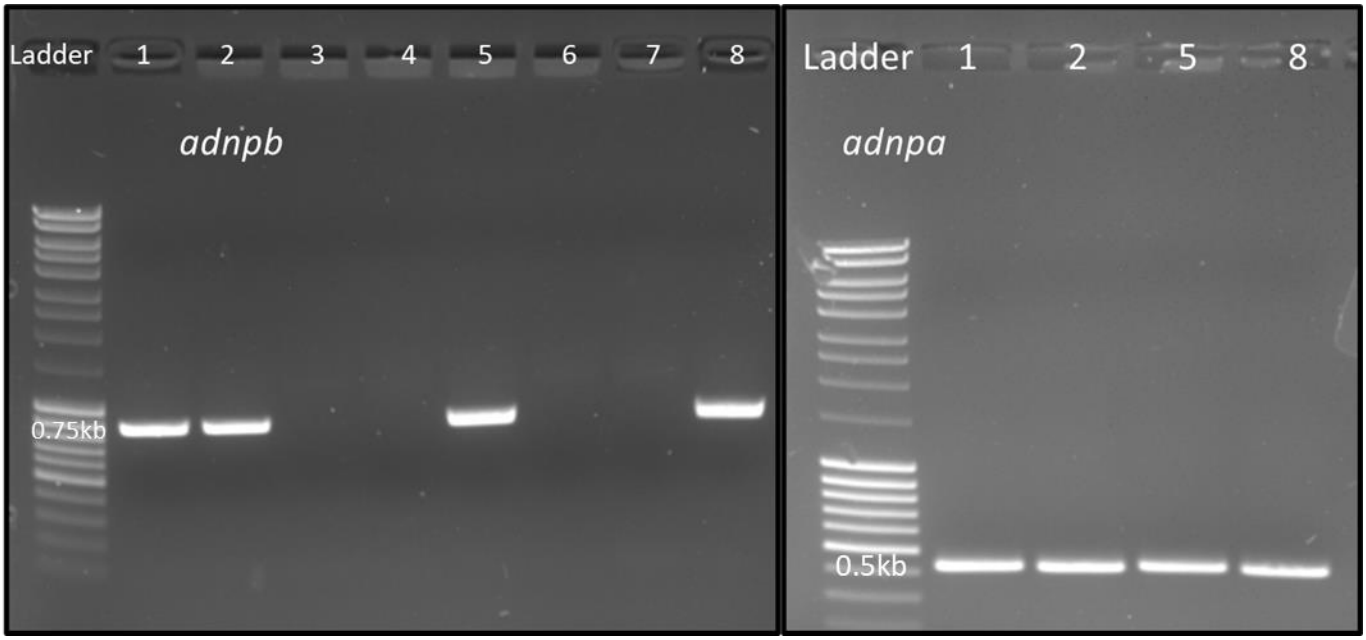

Figure 6: Representative gel image from genotyping strategy for *adnpa/b* double heterozygous fish. An *adnpa*$^{-/-}$ female and *adnpb* $^{+/-}$ male were crossed and 8 random embryos were sacrificed and genotyped at 24 hpf. Fish 1,2,5,8 which had the *adnpb* truncated allele were then genotyped for *adnpa* truncation. Consistent with expected mendelian ratios, 50% of the offspring were *adnpb*$^{+/-}$ and 100% were *adnpa* $^{+/-}$.

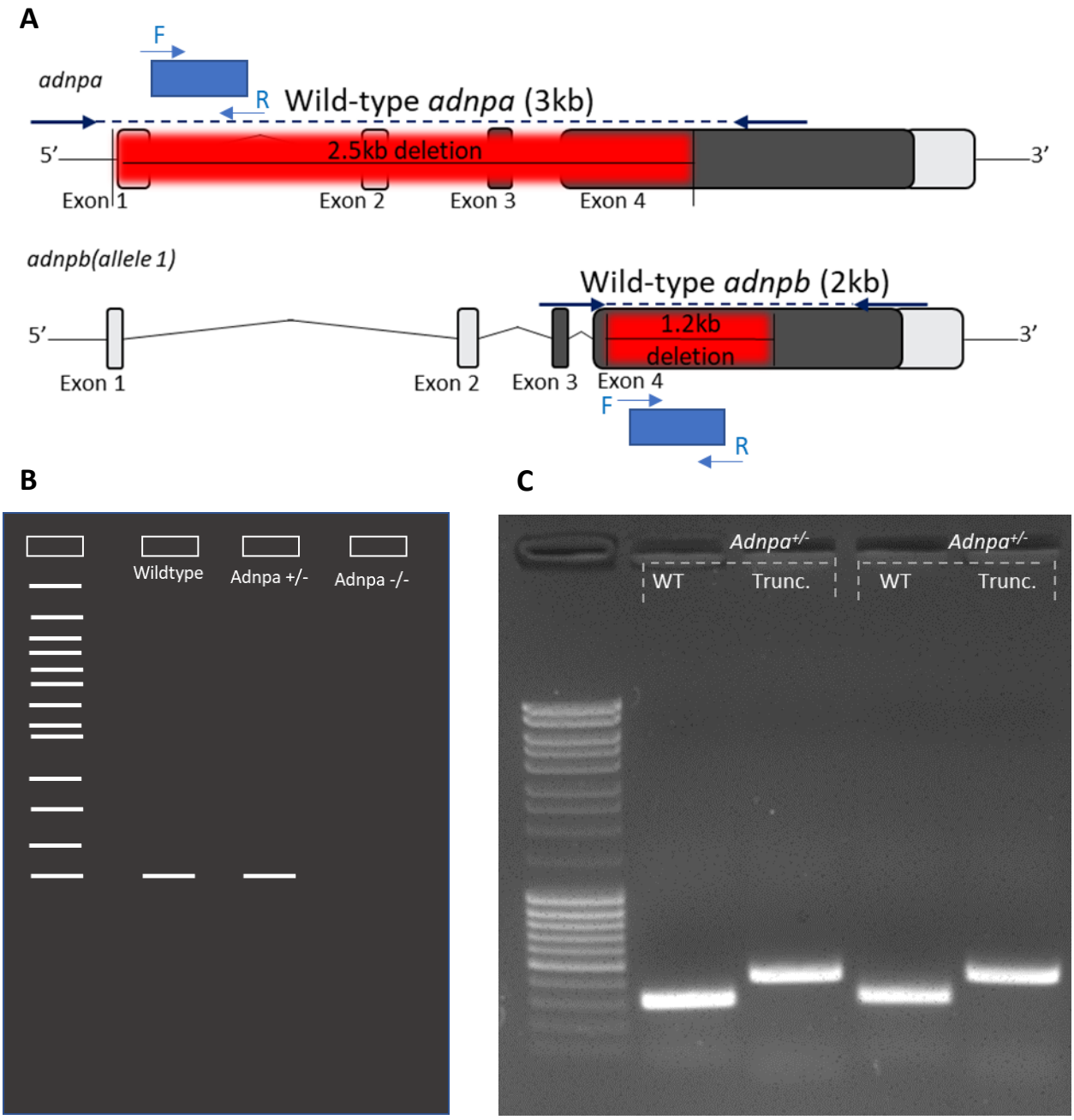

Figure 7: A) PCR Genotyping Primer Design for Distinguishing between Wildtype/Heterozygous and Homozygous alleles. PCR primers(blue) selectively amplify a region of exon 4 in *adnpa* and *adnpb* which is expected to be truncated in the mutant alleles. Thus this product will only amplify if the sample is wildtype or heterozygous. **B)** Graphical representation of gel product of

widtype, heterozygous and homozygous mutants using thes 'wildtype only' PCR primers. **C)** Representative gel image of amplification of heterozygous *adnpa* DNA using two primer sets, one which will amplify the truncated allele, and one which amplifies the wildtype allele. Taken together these were utilized to genotype and distinguish wildtype, heterozygous and homozygous mutants.

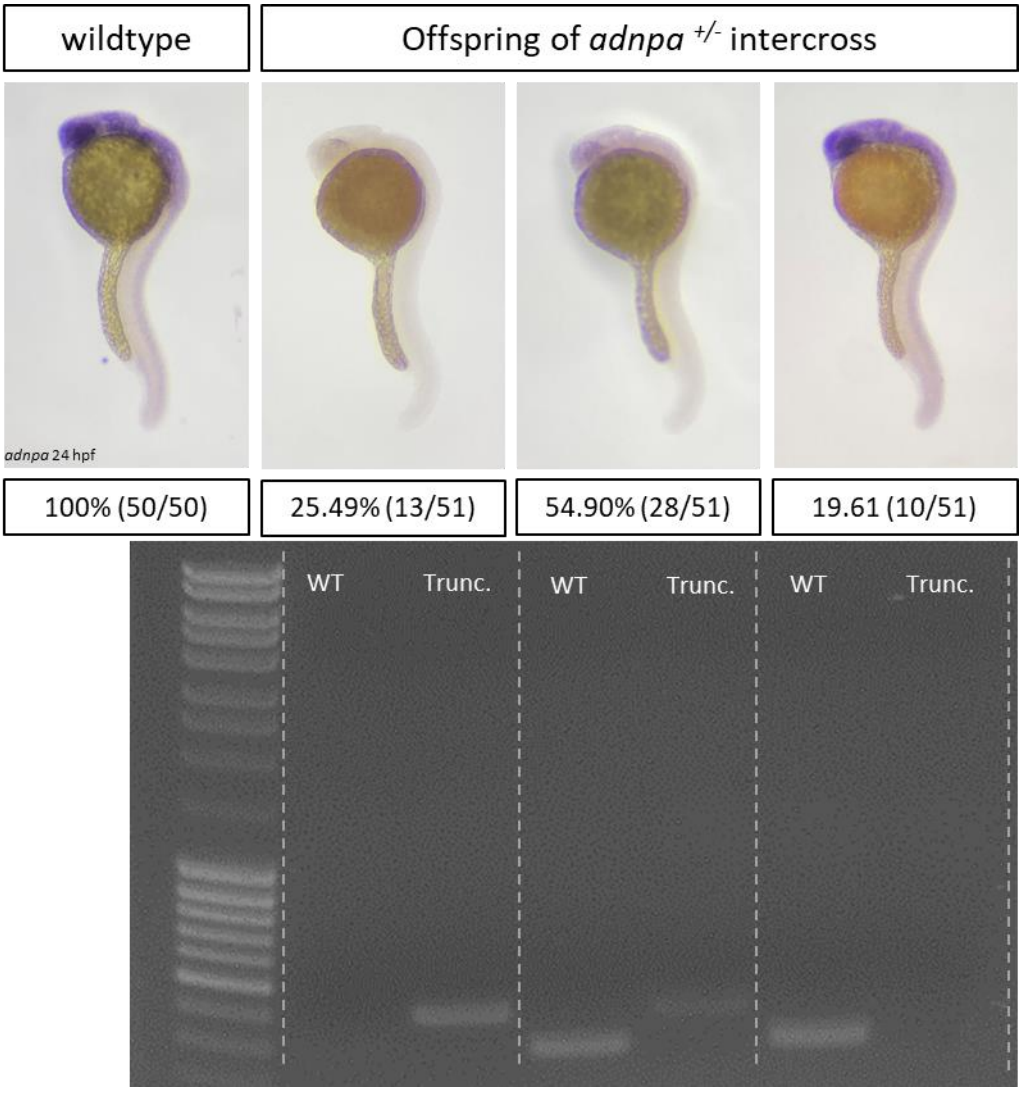

Figure 8: Representative images of whole mount *in situ* hybridization for *adnpa*, from left to right: wildtype, *adnpa* $^{-/-}$, *adnpa* $^{+/-}$, *adnpa* $^{+/+}$. Following imaging, DNA was extracted from the three embryos on the right and PCR genotyping was performed to confirm genotypes.

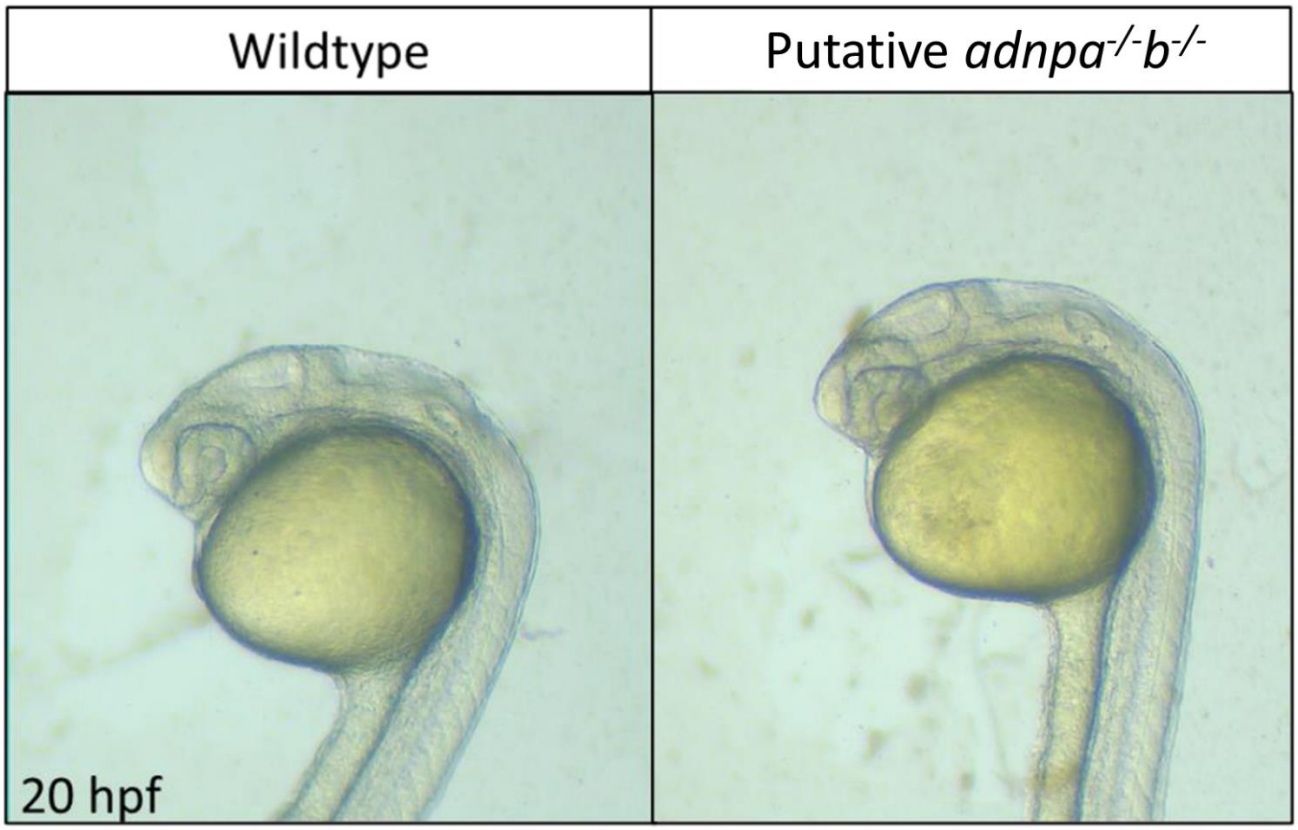

Figure 9: Representative images of wildtype and offspring of *adnpa*$^{+/-}$/*b*$^{+/-}$ intercross at 20 hpf.

No obvious changes in development were observed.

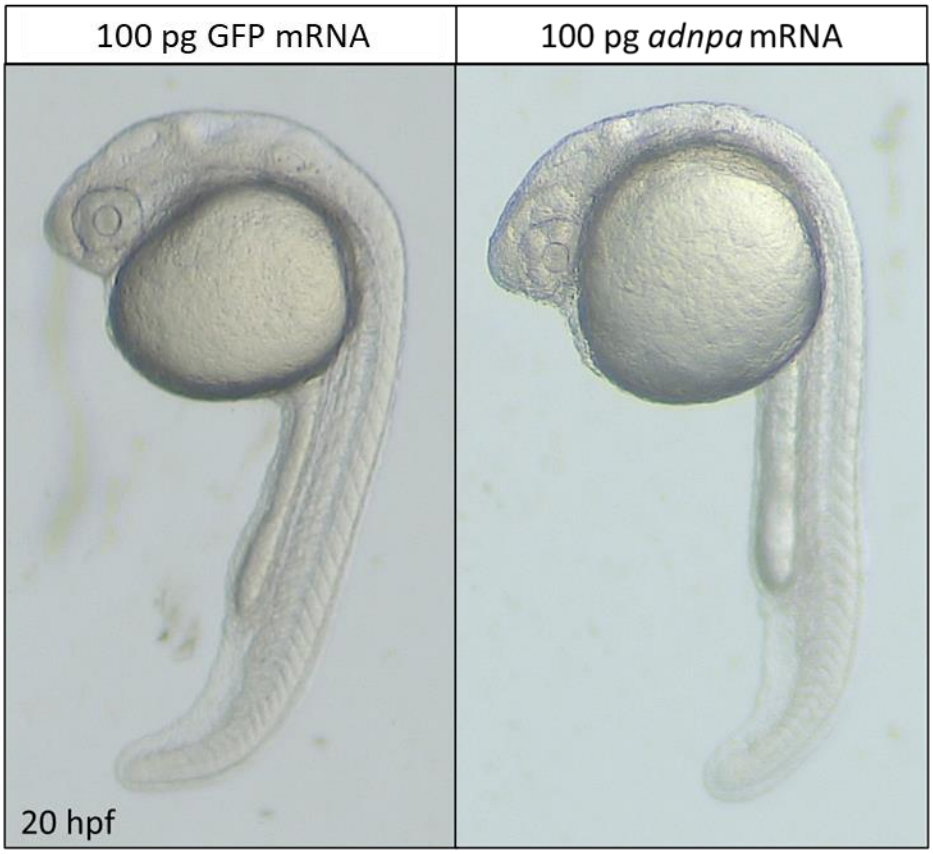

Figure 10: Representative images of embryo injected with 100 pg *adnpa* mRNA and 100 pg GFP control at 20 hpf. No changes in development were observed.

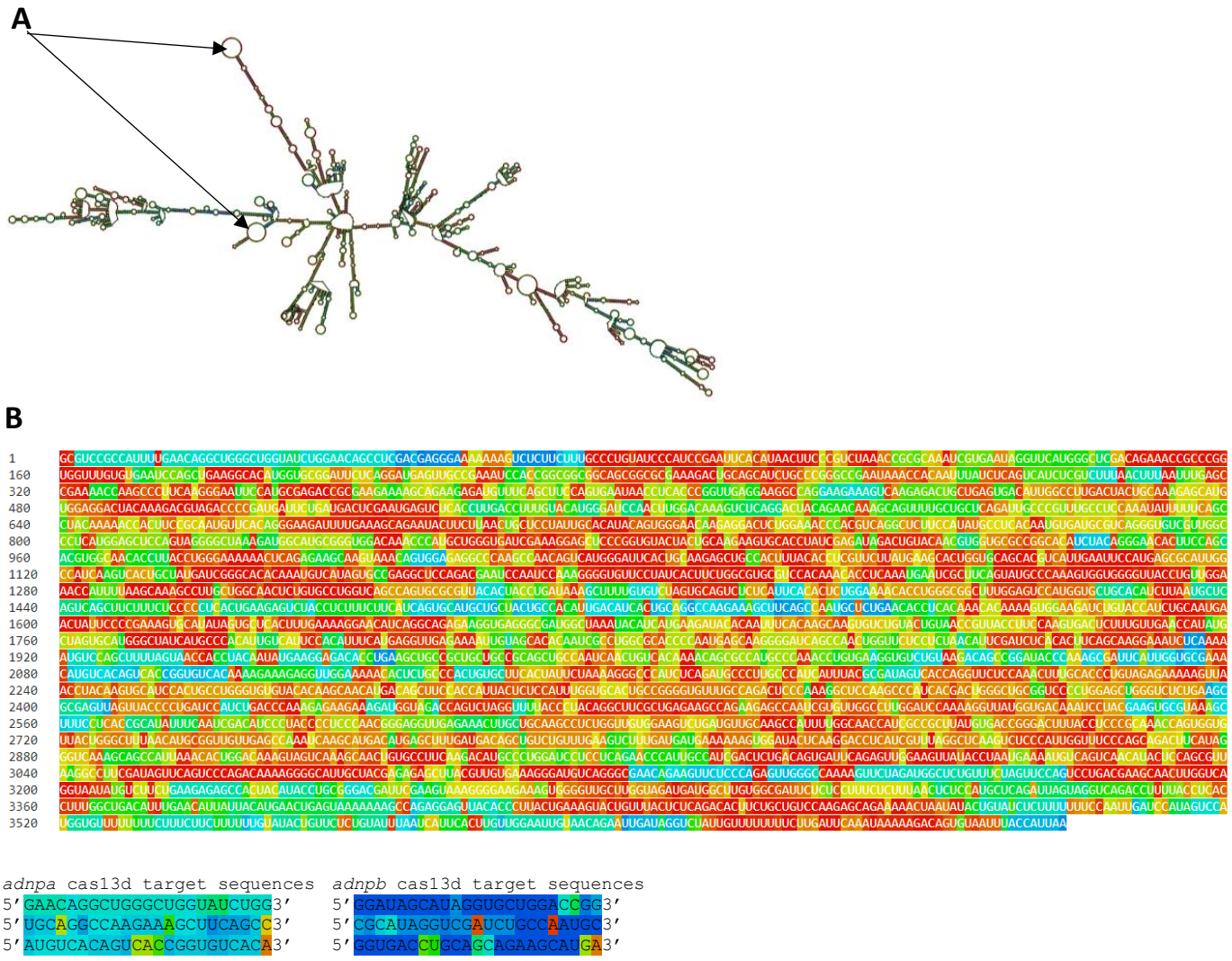

Figure 11: A) Image of the predicted secondary structure of *adnpa*. RNAs can form complex secondary structures with a mix of paired and unpaired bases. 23-mer regions of unpaired bases, such as those highlighted by arrows, are optimal targets for cas13d. **B)** Color coded base pairing probability for *adnpa* mRNA. Regions in dark/light blue represent low probability of base pairing. Orange/red represents high probability of base pairing. Cas13d sgRNA target sequences for *adnpa/b* are shown below the full sequence.

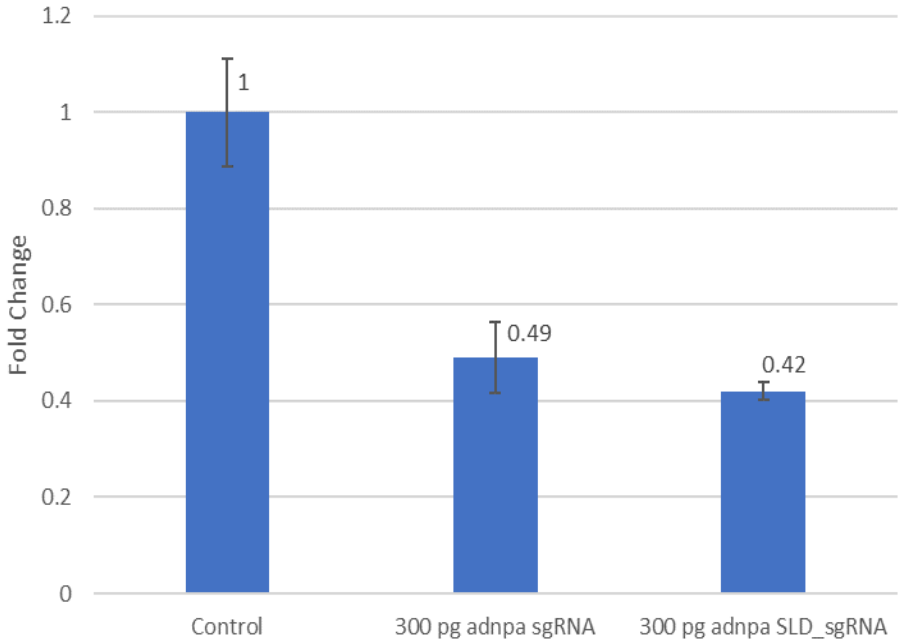

Figure 12: Results from qPCR of *adnpa* knockdown using CRISPR/Cas13d with the Standard Universal Primer sgRNAs and Stem-Loop Disruption Universal Primer (SLD_sgRNAs). The ΔCt values were calculated using *rpl13a* levels as the house keeping gene. ΔΔCt was calculated using cas13d-only control group ΔCt values. Fold change was calculated using $2^{-(\Delta\Delta Ct)}$, normalized to the cas13d-only control group. Results represent both biological and technical triplicates. Error bars shown in the figure represent standard deviation between each of the biological replicates.